



Effect of incident light and light gradients on eicosapentaenoic acid distribution between lipid classes in *Nannochloropsis oceanica*

Narcis Ferrer-Ledo¹ · Sabine van Oossanen^{1,2} · Rene H. Wijffels^{1,3} · Wendy A. C. Evers¹ · Christian Südfeld¹ · Marcel Janssen¹ · Iago Teles Dominguez Cabanelas¹ · Maria J. Barbosa¹

Received: 11 August 2024 / Revised: 10 October 2024 / Accepted: 14 October 2024
© The Author(s) 2024

Abstract

Commercial production of eicosapentaenoic acid (EPA) from photoautotrophic microalgae like *Nannochloropsis oceanica* requires higher productivity and larger scales to reduce costs. Improving productivity can be achieved by increasing biomass concentrations, which creates light gradients in the reactor depending on the culture's acclimation and the reactor geometry. These light gradients affect physiology, lipid synthesis, but also the distribution of fatty acids between lipid classes. In this study we evaluated the combined effect of the incident light intensity and light gradient on growth, biochemical composition, and fatty acid distribution between lipid classes. A total of 13 cultivations were performed in continuous mode using three different incident light intensities (200, 670, and 1550 $\mu\text{mol photons m}^{-2} \text{s}^{-1}$) and four dilution rates (from 0.29 to 0.75 day^{-1}). Reducing dilution rates resulted in higher biomass concentrations, steeper light gradients, and lower average light intensities. Increasing incident light intensity improved biomass productivity from 0.5 to 1.8 $\text{g L}^{-1} \text{day}^{-1}$, while the biomass yield on light decreased from 1.05 to 0.44 g mol^{-1} . Lowering average light intensities decreased the triglyceride content from 11.1 to 1.5% w/w, and increased the galactolipid content, mainly monogalactosyldiacylglycerol, up from 3.1 to 5.1% w/w. Total EPA contents did not decrease at low incident light but decreased by 28% at highly saturating light, both relative to medium incident light. The EPA content in polar lipids increased at lower average light intensities, and decreased in the neutral fraction simultaneously. These results highlight the tight regulation of EPA content between lipid polar and neutral fractions under different light regimes.

Keywords *Nannochloropsis oceanica* · Light intensity · Light gradient · Eicosapentaenoic acid · Lipidomics · Cyclostat

Introduction

Microalgae are regarded as a promising feedstock in the production of fuels, food, feed, and chemical ingredients (Draaisma et al. 2013). Despite the bright prospects, the

microalgae industry still needs to overcome high production costs in addition to relatively small production scales. As a result, microalgal products are limited to small market niches in the nutraceutical or cosmetic sectors (Enzing et al. 2014). Besides other commercially relevant compounds, microalgae produce lipids in high quantities with a unique fatty acid composition and distinct degrees of desaturation that cannot be found in other plant systems (Guschina & Harwood 2006; Hess et al. 2018). Omega-3 fatty acids (n-3 FAs) comprise a class of monounsaturated and polyunsaturated fatty acids (PUFAs) known for their involvement in several physiological processes such as neuronal development (Dyall & Michael-Titus 2008) or modulation of inflammation (Bhatt et al. 2019). Several microalgae accumulate high amounts of n-3 FA and their lipids could be used as ingredients in diets for fish and humans. Additionally, microalgae-derived n-3 FAs hold the potential to substitute fish or krill oil, the current

N. Ferrer-Ledo and S. van Oossanen contributed equally to this manuscript.

✉ Maria J. Barbosa
maria.barbosa@wur.nl

¹ Bioprocess Engineering, AlgaePARC, Wageningen University and Research, P.O. Box 16, 6700 AA Wageningen, The Netherlands

² Laboratory of Systems and Synthetic Biology, Wageningen University & Research, 6708 WE Wageningen, The Netherlands

³ Faculty of Biosciences and Aquaculture, Nord University, N-8049 Bodø, Norway

sources of n-3 FA of which the use has been questioned in the last years (Jenkins et al. 2009; Adarme-Vega et al. 2012).

Nannochloropsis oceanica is an unicellular marine microalgal species, that belongs to the class of the Eustigmatophyceae. Species from the genus *Nannochloropsis* can inhabit a wide range of environments (freshwater, brackish, and marine waters), grow relatively fast, and can accumulate high amounts of lipids, especially LC-PUFAs (Griffiths & Harrison 2009; Janssen et al. 2018). Additionally, the increasing availability of genomic information (Gong et al. 2020) and genetic tools (Naduthodi et al. 2018) together with the large experience in outdoor conditions (Chini Zittelli et al. 1999; de Vree et al. 2016) convert this species into an interesting single-cell oil platform for food, feed, and fuel applications (Al-Hoqani et al. 2017).

Nannochloropsis species are especially well-known for accumulating high quantities of the n-3 fatty acid, eicosapentaenoic acid (EPA; C20:5). EPA can be found either esterified in phospholipids, betaine lipids, or glycolipids (polar fraction), or triacylglycerols (TAG) (neutral fraction). EPA localization between the fractions depends on environmental stimuli (Janssen, et al. 2019a, b). Based on the differing EPA content of neutral and polar lipids, the downstream route for the extraction of EPA and possibly the final application might differ (Sijtsma & De Swaaf 2004). For example, an oil rich in TAG could be of interest for energy and bulk chemical applications (Hu et al. 2008), while an oil rich in phospholipids and galactolipids would be more suitable for nutraceutical, cosmetic, and feed applications (Traversier et al. 2018).

In phototrophic eukaryotes, the chloroplast is the organelle responsible for light absorption and carbon fixation. Light capture and electron transfer occur throughout the cooperative work of photosystems I and II, which in eukaryotes are found embedded in the thylakoids. Thylakoid membranes are organized in stacked structures (grana) with a high presence of PSII or in unstacked structures (stroma lamellae) connecting the grana with enriched amounts of PSI and ATPases (Staehelin 2003). The organization of the thylakoid membranes and photosystems is very malleable and sensitive to the light regime (Pribil et al. 2014). On the one hand, low light intensities favour an increase of photosystems and light-harvesting complexes (LHC) to maximize the absorption of light into photochemistry. In response, microalgae increase chloroplast membranes, and therefore the formation of new stacks of grana. On the other hand, light intensities that exceed the light required for photochemistry lead to the generation of reactive oxygen species (ROS) with consequent damage to membranes and growth impairment. Cells limit the damage by decreasing the degree of grana stacking, redistributing the antenna between PSII and PSI, and reorganizing PSII-LHC complexes. Those

mechanisms ultimately aim to dissipate the excess energy and facilitate the repair of damaged PSII (Liu et al. 2019).

The lipid fraction in the thylakoids accounts only for 30% of the thylakoid mass (Kirchhoff et al. 2002) and includes the galactolipids monogalactosyldiacylglycerol (MGDG; 15–47%), digalactosyldiacylglycerol (DGDG; 11–20%), sulfoquinovosyldiacylglycerol (SQDG; 7–29%), and a minor fraction of the phospholipid phosphatidylglycerol (PG; 2–10%) (Li-Beisson et al. 2019). Despite the low content of lipids in the thylakoids, EPA was reported to be highly present in the galactolipid fraction and to a lesser extent, in phospholipids (Sukenik et al. 1989). Since the light intensity can influence the lipid architecture of the chloroplast, it is important to gain an understanding of how EPA distribution is affected by the light gradient. The FA accumulation and composition in *Nannochloropsis* species have been extensively studied by several authors mainly as a function of the incident light intensity (Renaud et al. 1991; Sukenik et al. 1993; Fabregas et al. 2003). Nevertheless, the distribution of the fatty acids, and especially EPA, between lipid classes in *Nannochloropsis* species has been only researched in a few studies. Sukenik and co-workers (1989) reported a negative correlation between the light intensity and the synthesis rate of galactolipids while the correlation was positive for the synthesis of TAG. Similar observations were reported for galactolipids and TAG in subsequent work, with new insights into the role of phospholipids (Han et al. 2017) and the betaine lipid diacylglyceryltrimethylhomo-serine (DGTS) (Alboresi et al. 2016).

Light is usually the limiting factor in phototrophic cultivations. Light does not dissolve in the reactor, such as organic substrates, but instead attenuates over the reactor depth. Consequently, cells experience a light gradient which has large implications for their photosynthetic efficiency and growth (Janssen et al. 2001). The nature of this light gradient is especially important in outdoor cultivations since high growth rates coupled with high biomass concentrations are desired to achieve high biomass productivities. The shape of the gradient is highly influenced by the biomass concentration and will determine the integral growth and lipid synthesis rates. For instance, dense cultures will lead to dark zones, which could favour the redox turnover of the plastoquinones involved in photosynthesis and potentially help in the repair of the photodamaged reaction centres (Polle & Melis 1999). Experiments with optically thin cultures concluded that adequate dynamics of cells between light and dark cycles could lead to higher photosynthetic performances (Qiang & Richmond 1996; Janssen et al. 2000; Barbosa et al. 2003; Olivieri et al. 2015). Independently of the length of the dark and photic zones, the characteristics of the light gradients on the culture can be assessed with the concept of the average light intensity (I_{av}) (Rabe & Benoit 1962; Molina Grima et al. 1999). This parameter is important for outdoor

operations since it provides information on the light that the culture is directly experiencing (Richmond & Hu 2013). Several studies have used the I_{av} to characterize the growth kinetics of microalgae (Molina Grima et al. 1999, 1996; Koller et al. 2017) to define the optimal light growth conditions (Pfaffinger et al. 2016). Nevertheless, much less is known about how I_{av} and the interplay between I_{av} and the incident light intensity at the culture surface ($I_{ph,0}$) affects biomass growth and synthesis of high-value products such as EPA.

In this study we investigated the effect of different incident light intensities (200, 670, and 1550 $\mu\text{mol photons m}^{-2} \text{s}^{-1}$) and light gradients (i.e., biomass concentrations) on the growth, lipid, and pigment accumulation of *Nannochloropsis oceanica*. A total of 13 cyclostat experiments were done in laboratory-scale flat panel photobioreactors at dilution rates ranging from 0.3 to 0.7 day^{-1} . The dilution rate determined the biomass concentration which, together with the absorbing and light scattering properties of the culture, generated a light gradient of a certain average light intensity. Photosynthetic efficiencies and biomass productivities were assessed and intercorrelated to changes in lipids and pigment characteristics. The lipid class composition of the lipid fraction and changes in the fatty acyl moieties were evaluated to infer the lipid response under different light conditions. Finally, the EPA content and its distribution between fractions were analysed to gain an understanding of how EPA is modulated by the incident light intensity and light gradient.

Materials and Methods

Strain, medium, and pre-cultivation conditions

Nannochloropsis oceanica was kindly provided by NEC-TON S.A. (Olhão, Portugal). Pre-cultures were incubated in 250 mL shake flasks containing 100 mL of filter-sterilised medium (pore size 0.2 μm). The growth medium of precultures contained the following composition, adapted from NutriBloom Plus (Phytobloom, Olhão, Portugal): NaCl 419.2 mM; $\text{MgCl}_2 \cdot 6\text{H}_2\text{O}$ 48.2 mM; NaNO_3 35.3 mM; Na_2SO_4 22.5 mM; $\text{CaCl}_2 \cdot 2\text{H}_2\text{O}$ 5.4 mM; K_2SO_4 4.9 mM; KH_2PO_4 0.7 mM; $\text{Na}_2\text{EDTA} \cdot 2\text{H}_2\text{O}$ 52.8 μM ; $\text{FeCl}_3 \cdot 6\text{H}_2\text{O}$ 40.0 μM ; $\text{ZnSO}_4 \cdot 7\text{H}_2\text{O}$ 4.0 μM ; $\text{MgSO}_4 \cdot 7\text{H}_2\text{O}$ 4.0 μM ; $\text{MnCl}_2 \cdot 4\text{H}_2\text{O}$ 2.0 μM ; $\text{Na}_2\text{MoO}_4 \cdot 2\text{H}_2\text{O}$ 0.2 μM ; $\text{CoCl}_2 \cdot 6\text{H}_2\text{O}$ 0.2 μM ; $\text{CuSO}_4 \cdot 5\text{H}_2\text{O}$ 0.2 μM . HEPES was added at a final concentration of 20.0 mM and pH was adjusted to 7.5 using 2.5 M HCl and 2.5 M NaOH solutions. Maintenance cultures were incubated in climate-controlled chambers in an orbital shaker (90 rpm) at 25 °C and 50 $\mu\text{mol photons m}^{-2} \text{s}^{-1}$ of incident light with a diurnal cycle (L:D) of 16:8. Pre-cultures for reactors were incubated in an orbital shaker HT Multi-tron Pro (Infors HT, Switzerland) at 25 °C, with a rotational

speed of 120 rpm, light intensity of 150 $\mu\text{mol photons m}^{-2} \text{s}^{-1}$ (warm-white LED), a CO_2 enriched atmosphere (0.2%), and 16:8 h light:dark photoperiod.

The composition of the medium used in the reactors was the same except that HEPES was not added. To prevent any nutrient limitations, concentrations of NaNO_3 and KH_2PO_4 were increased to 58.8 and 2.76 mM for the continuous experiments at high incident light intensities. Besides, the pH of the modified medium was adjusted to 6 to prevent nutrient precipitation in the medium during storage.

Experimental set-up and photobioreactor operation

Experiments were performed in heat-sterilised airlift-loop flat panel Labfors 5 photobioreactors (Infors HT, Switzerland) operated in cyclostat mode by switching on the dilution rate during the light period and switching off the dilution during the dark period. Reactors have a working volume of 1.8 L, a depth of 20.7 mm, and an illuminated surface area of 0.08 m^2 . Mixing of the culture was provided with air at 0.56 vvm enriched with 2% CO_2 . Temperature was maintained at 25 °C and controlled through a water jacket with recirculating water connected to a cryostat. pH was maintained at 7.5 ± 0.1 and controlled with the addition of base (1 M NaOH) or acid (0.9 M H_2SO_4). Incident light was provided by 260 water-cooled and high-power LEDs (28 V, 2.3 W). Light intensity changed in a block form with a light period of 16 h of light and 8 h of dark. A condenser (4–10 °C) was used to minimise evaporation losses from the culture. The medium was continuously fed to the reactor with a pre-calibrated pump that was remotely controlled by a central PC unit (Infors HT, Switzerland). Reactor dilution stopped during the night. The volume in the reactor was kept constant by continuously pumping out surplus broth above the working volume.

Reactors were operated at three different incident light intensities ($I_{ph,0}$): 200 $\mu\text{mol photons m}^{-2} \text{s}^{-1}$ (LL), 670 $\mu\text{mol photons m}^{-2} \text{s}^{-1}$ (ML), and 1550 $\mu\text{mol photons m}^{-2} \text{s}^{-1}$ (HL). Cultures were inoculated at an optical density (OD_{750}) of 0.15–0.20 and operated in batch mode at an initial $I_{ph,0}$ of 200 $\mu\text{mol photons m}^{-2} \text{s}^{-1}$. In the ML and HL experiments, the light was increased stepwise before reaching the setpoints of 670 $\mu\text{mol photons m}^{-2} \text{s}^{-1}$ and 1550 $\mu\text{mol photons m}^{-2} \text{s}^{-1}$. Once dilution of the cultures started, dry weight (DW) and absorption cross-section (a_x) were used as the physiological parameters to assess the stability of the culture. Cultures were considered at a steady state when DW and a_x were constant (less than 10% change) after 3 complete replacements of the reactor volume. Four dilution rates (D) were applied at LL and ML (0.75 day^{-1} , 0.6 day^{-1} , 0.45 day^{-1} , 0.29 day^{-1}) and two dilution rates at HL (0.67 day^{-1} and 0.36 day^{-1}). The experiment with the highest I_{av} (1000 $\mu\text{mol photons m}^{-2} \text{s}^{-1}$) followed a slightly different

approach. A turbidostat operation mode was applied to reach steady growth at an I_{av} of 1000 $\mu\text{mol photons m}^{-2} \text{s}^{-1}$ and then switched to cyclostat mode using the same dilution rate as reached during the turbidostat phase.

Offline reactor measurements

Samples were always collected exactly 2 h into the light period. Samples taken directly from the reactor were used to measure optical density, dry weight, absorption cross-section, and maximum quantum yield (QY). Light on the backside of the reactor ($I_{ph,d}$) was measured with a light meter (LI-190SA 2 π PAR quantum sensor, LI-COR, USA) and averaged over 24 equally distributed points of the reactor surface. The overflow was collected in an empty vessel stored in the dark on ice water, starting from the time of reactor sampling. The overflow from the reactor was collected for 4 h. The harvested overflow was centrifuged (5 min, 4000 $\times g$ at 4 °C), and the resulting pellet was washed twice with ammonium formate (0.5 M) to remove the excess salts. After the second washing step, the pellet was frozen at -20 °C and subsequently freeze-dried. The lyophilized pellet was ground, flushed with N₂ gas, and stored at -20 °C until further use. At least three samples were collected on different days during steady state.

Sample analysis

Dry weight (DW, g L⁻¹) was measured gravimetrically. Glass microfiber filters (Whatman GF/F, 55 mm; GE Healthcare, USA) were dried at 100 °C overnight, cooled down to room temperature in a desiccator, and weighed. A volume of culture containing 2–5 mg of wet biomass was filtered and washed with ammonium formate (0.5 M) to remove the salts from the culture samples. Filters were dried in the oven for at least 24 h, cooled in the desiccator, and weighed. Measurements were done in triplicate.

The maximum quantum yield (QY) of the culture was measured with a fluorometer AquaPen AP-C100 (Photon Systems Instruments, Czech Republic). Samples with an OD₇₅₀ ranging from 0.2–0.5 were incubated for 10–15 min in the dark. A short and highly saturating pulse of blue light (455 nm) was used to measure the maximum fluorescence (F_m) after measuring the baseline fluorescence without photosynthetic light (F_o). The efficiency of the photosystems was calculated as follows:

$$QY = \frac{F_m - F_o}{F_m} \quad (1)$$

The specific absorption cross-section (a_x , m² kg⁻¹) was measured by using a UV-2600/2700 spectrophotometer (Shimadzu, Japan) equipped with an integrating sphere to correct

for light scattering. The absorption spectrum from 400 to 750 nm of undiluted samples was measured and normalised by the path length (2 mm) and dry weight concentration. The specific optical cross-section was then normalised by the absorbance between 740 and 750, which is considered to be residual scattering and averaged from 400 to 700 nm.

Pigment extraction and quantification were performed as described by Barten et al. (2021). Briefly, a mixture of 5–10 mg of freeze-dried biomass with 1.5 mL 0.1% butylhydroxytoluene/methanol solution was bead-beaten (3 \times 90 s at 5000 rpm with a 45-s break), centrifuged (3 min, 16,000 rpm) and the supernatant was collected in a glass tube. The lipid extraction step was repeated 5 more times, each time adding a fresh solution of 0.1% butylhydroxytoluene/methanol. For detecting canthaxanthin and astaxanthin, the solvents were replaced by evaporating the methanol mixture and adding acetone or methyl-tert-butyl-ether respectively. Standard curves were prepared for analytical standards of chlorophyll *a*, astaxanthin, antheraxanthin, violaxanthin, zeaxanthin, and β -carotene (Carotenature, Switzerland). Pigment extracts were separated and analysed by High-Performance Liquid Chromatography (HPLC) with a Shimadzu (U)HPLC system (Nexera X2, Shimadzu, Japan). Detailed operating conditions are as described by Barten et al. (2021). Vaucherixanthin was detected and quantified based on retention times and extinction spectra found in literature (Jeffrey et al. 1997; Keşan et al. 2016).

Fatty acid (FA) quantification between lipid classes started with the disruption of 5–10 mg of freeze-dried biomass for lipid extraction. The extraction was done according to Breuer et al. (2013) with the exception that no standard was added during the extraction with the chloroform: methanol solution (4:5). From the lipid extract, a representative sample of 50 μL was taken to convert the fatty acids into methyl esters (FAMES) by one-hour incubation at 100 °C with 3 mL of a solution containing FA standard, 5% H₂SO₄, and methanol. As a FA standard, pentadecanoic acid (CAS 1002–84–2, Merck, Germany) was added for the FA quantification. The methylation reaction was stopped by adding 3 mL deionised water and 1 mL hexane. Subsequently, the FAMES in the hexane were analysed by Gas Chromatography-Flame Ionisation Detection (GC-FID, 7890B, Agilent Technologies, US). From the remaining lipid extract, the lipid classes were separated by Thin Layer Chromatography (TLC) as described by Gros and Jouhet (2018), with some minor modifications. For the TLC analysis, a total of 200 μg of total fatty acids (TFAs) from the lipid extract were loaded on a pre-coated and preactivated TLC silica plate (105,721, Supelco, Germany) and were migrated according to the protocol guidelines (Gros & Jouhet 2018). In short, neutral lipids were fractionated by running TLC in one dimension while polar lipids were fractionated by running TLC in two dimensions. The migration solution for neutral lipids

separation consisted of hexane: diethyl ether: acetic acid at a 70:30:1 ratio. For polar lipids, migration solution for the first dimension consisted of chloroform:methanol: deionised water at a ratio of 65:25:4. Migration solution for the second dimension consisted of chloroform:acetone:methanol: acetic acid: deionised water at a ratio of 50:20:10:10:5. After drying the plates under continuous nitrogen flushing, a solution of primuline 0.5% w/v (CAS 8064–84-2, Merck, Germany) in 8:2 acetone: deionised water was sprayed onto the silica plates. Lipid class spots were identified under a UV inspection cabinet (CAMAG, The Netherlands) with UV irradiation at 366 nm. The identification of the lipid classes was set up in consultation with the Laboratoire de physiologie cellulaire et végétale (Grenoble, France), which previously characterised the lipidome of *Nannochloropsis* species using GC–MS. The identification of lipid classes on silica plates is represented in Fig S2. The FAs in the lipid classes were quantified by scraping and collecting the lipid-containing silica spots from the TLC plate in a glass tube, methylating the lipid classes, and measuring the FA content using GC-FID. The GC (7890B, Agilent Technologies, USA) was operated as described by Breuer et al. (2013) with the exception that hydrogen was used as the gas carrier. Additionally, the total flow rate was adjusted to 44 mL min⁻¹ and the initial oven temperature was held for 0.23 min, then raised by 44 °C min⁻¹. The total run time per sample was adjusted to 25 min. To quantify the GC readings, the relative response of a standard mix of fatty acid methyl esters (FAMES) was used. FA contents in biomass were normalised to the initial weighted DW. To estimate the FA distribution per lipid class (% mol mol⁻¹), the content of each FA in a lipid class was normalised to the sum of the total FAs in the lipid class. In turn, the lipid class distribution was calculated as the ratio of the total FA content found in each lipid class spot over the sum of the combined FA contents in all lipid classes, taking into account the number of acyl chains per lipid class. While overall TFA per sample was quantified for all replicates, the lipid class composition was measured for a limited number of samples. Lipid class composition was measured for each replicate of the reactor runs at the highest and lowest I_{av} , and for single replicates of reactor runs at intermediate I_{av} . The relative shift in lipid class FA distributions, resulting from both increased incident and average light conditions, was quantified by taking the FA content ratio between the highest and lowest I_{av} for each incident light level.

Rates and reactor calculations

The dilution rate (D , day⁻¹) was calculated based on the total volume of the reactor and the overflow volume collected after 24 h as follows:

$$D = \frac{V_{harvest}}{V_r} \quad (2)$$

where $V_{harvest}$ (L) is the overflow volume harvested after 1 day and V_r (L) is the working volume of the reactor. The average light intensity (I_{av}) was calculated by integrating the light path over the depth of the reactor as follows:

$$I_{av} = \frac{1}{d} \cdot \int_0^d I_{ph,0} \cdot e^{(-\varepsilon \cdot z)} \cdot dz = \frac{I_{ph,0}}{\varepsilon \cdot d} \cdot (1 - e^{(-\varepsilon \cdot d)}) \quad (3)$$

where d is the total depth of the light path (m), $I_{ph,0}$ is the incident light intensity ($\mu\text{mol photons m}^{-2} \text{s}^{-1}$), ε stands for the light attenuation coefficient ($\text{m}^2 \text{L}^{-1}$) and z stands for the length at any point of the reactor depth (m). The light attenuation coefficient was calculated by Lambert–Beer's law:

$$\varepsilon = \frac{\ln\left(\frac{I_{ph,0}}{I_{ph,d}}\right)}{d} \quad (4)$$

where $I_{ph,d}$ stands for the light measured on the rear of the reactor ($\mu\text{mol photons m}^{-2} \text{s}^{-1}$). The $I_{ph,d}$ values were adjusted to account for light divergence and reflection losses in the water jacket by incorporating a correction factor, $I_{blank}/I_{ph,0}$. In this context, I_{blank} represents the light intensity measured at the rear of the reactor when only medium is present, and $I_{ph,0}$ represents the light intensity measured after the first glass plate from the perspective of the light source. Correction factors used in this study varied between 0.80–0.86, depending on the reactor vessel.

The biomass-specific photon absorption rate ($q_{ph,abs}$, mmol g_{DW}⁻¹ h⁻¹) was calculated as follows:

$$q_{ph,abs} = \frac{(I_{ph,0} - I_{ph,d})}{C_x \cdot d} \quad (5)$$

The volumetric biomass productivity (r_x , mg L⁻¹ day⁻¹) and light absorption rate ($r_{ph,abs}$, mol L⁻¹ day⁻¹) are defined as

$$r_x = DC_x \quad (6)$$

$$r_{ph,abs} = \left(\frac{I_{ph,0} - I_{ph,d}}{d}\right) \cdot 16 \quad (7)$$

where 16 stands for the number of hours of light per day. The observed yield of biomass on light (Y_{xph} , g mol⁻¹) is defined as

$$Y_{xph} = \frac{r_x}{r_{ph,abs}} \quad (8)$$

The illuminated fraction (ϵ) was calculated based on the reactor depth z_c where light intensity equals the compensation point of photosynthesis the $I_{ph,c}$:

$$z_c = \frac{\ln\left(\frac{I_{ph,0}}{I_{ph,c}}\right)}{C_x a_x S} \quad (9)$$

$$\epsilon = \frac{z_c}{d} \quad (10)$$

calculated compensation point $I_{ph,c}$ was 4.0 $\mu\text{mol photons m}^{-2} \text{s}^{-1}$ based on the specific light requirement of 3.5 $\text{mmol g}_{\text{DW}}^{-1} \text{h}^{-1}$ obtained by Barten et al. (2022) and an a_x of 250 $\text{m}^2 \text{kg}^{-1}$. Parameter S is a correction factor accounting for light scattering and was obtained individually for each steady state condition according to:

$$S = \frac{\ln\left(\frac{I_{ph,0}}{I_{ph,d}}\right)}{C_x a_x d} \quad (11)$$

Statistical analysis

Each steady state was analysed with descriptive statistics by calculating the mean and the standard deviation of three replicates. Analysis of variance (ANOVA) was used to assess the significance of changes in biomass yields, productivities, and lipid contents at different average light intensities with a confidence level of 95%. Homoscedasticity of the different groups was assessed by applying Levene's test with a confidence level of 95%. The significance of changes in FA composition between different incident light conditions was assessed with the post-hoc Tukey's range test with a confidence level of 95%. Propagation of error was also applied when arithmetic operations were involved. Statistical treatments were carried out using R (R Core Team), and data was visualised with Matlab (The MathWorks, Inc.).

Results and Discussion

Incident light and average light intensity affect growth

The average light intensity (I_{av}) represents the spatial average light intensity received by the culture. The I_{av} is therefore dependent on the incident light, the depth of the reactor, the biomass concentration, and the absorbing and scattering properties of the algal cells. In this study, the dilution rate (D) was used to vary the biomass concentration and therefore to obtain different light gradients across the reactor depth. Applying varying light gradients in addition to varying incident light intensities ($I_{ph,0}$) resulted in a range of I_{av} values that could be used to study how algal growth and lipid accumulation were affected by the I_{av} and how both could be controlled by the dilution rate. We applied the

incident light intensities of 200 $\mu\text{mol photons m}^{-2} \text{s}^{-1}$ (LL), 670 $\mu\text{mol photons m}^{-2} \text{s}^{-1}$ (ML), and 1550 $\mu\text{mol photons m}^{-2} \text{s}^{-1}$ (HL), representing sub-saturating, saturating, and over-saturating light conditions respectively. LL and ML were selected based on previous studies where saturating light intensities of 210 and 538 $\mu\text{mol photons m}^{-2} \text{s}^{-1}$ were found at low and high light conditions, respectively (Suke-nik 1991; Fisher et al. 1996; Pfaffinger et al. 2016). The HL intensity was selected based on representative incident light intensities found in outdoor conditions in Algarve (Fig S3, Table S1.A, Table S1.B). A range of four dilution rates (D) was set. The highest D was chosen to be 0.81 day^{-1} , based on the highest observed growth rate in reactor cultivations of *Nannochloropsis* spp. (Suke-nik 1991) while the lowest D was chosen to be 0.29 day^{-1} .

With decreasing D at LL, ML, and HL, the biomass dry weight (DW) increased from 0.50 to 1.77 g L^{-1} , 1.60 to 3.78 g L^{-1} , and 2.75 to 4.41 g L^{-1} , respectively (Fig. 1A). The increase in biomass concentrations with rising $I_{ph,0}$ settings suggests that light was a limiting factor over the range of D conditions studied. Nevertheless, the increase in biomass DW from LL to ML was less prominent when $I_{ph,0}$ was increased to HL, indicating an inhibitory effect on growth. As expected, the increase in biomass concentrations led to a decrease in I_{av} . This decrease occurred with each incremental reduction in dilution rate (Fig. 1B). The I_{av} decreased from 115 to 41 $\mu\text{mol photons m}^{-2} \text{s}^{-1}$ at LL, while for ML and HL, the I_{av} decreased from 245 to 78 $\mu\text{mol photons m}^{-2} \text{s}^{-1}$ and 457 to 175 $\mu\text{mol photons m}^{-2} \text{s}^{-1}$, respectively. The decrease in I_{av} over the biomass concentration becomes sharper when moving to increased incident light intensity, as seen by comparing the HL curve to LL and ML in Fig. 1B.

Due to the more than probable photoinhibitory effect at high light saturating conditions, the experiment was repeated at an average light intensity (I_{av}) of 957 $\mu\text{mol photons m}^{-2} \text{s}^{-1}$ following a slightly different approach. First, a turbidostat setup (HL-tbstat) was used to reach an I_{av} close to 1000 $\mu\text{mol photons m}^{-2} \text{s}^{-1}$ at HL, validating the ability of *N. oceanica* to grow at highly light-saturating conditions. Then, the culture was maintained in cyclostat mode, similar to the LL and ML experiments. The biomass concentration and D resulting from the turbidostat were 0.84 g L^{-1} and 0.58 day^{-1} , respectively. A comparison between the HL-tbstat dataset with other HL datasets shows a deviation from the trend of the increasing biomass concentrations with increasing $I_{ph,0}$, which is a possible effect of photoinhibition at HL. At high I_{av} , light is absorbed in excess due to an increased light supply rate (Table S2). The incapacity to safely dissipate the excitation energy from the photosystems led to photoinhibition of the PSII and a reduction in growth. This was confirmed by a low QY (0.44) which deviated notably from the other experimental conditions (Table S2). In the reactor runs at LL, ML, and HL, the QY decreased from

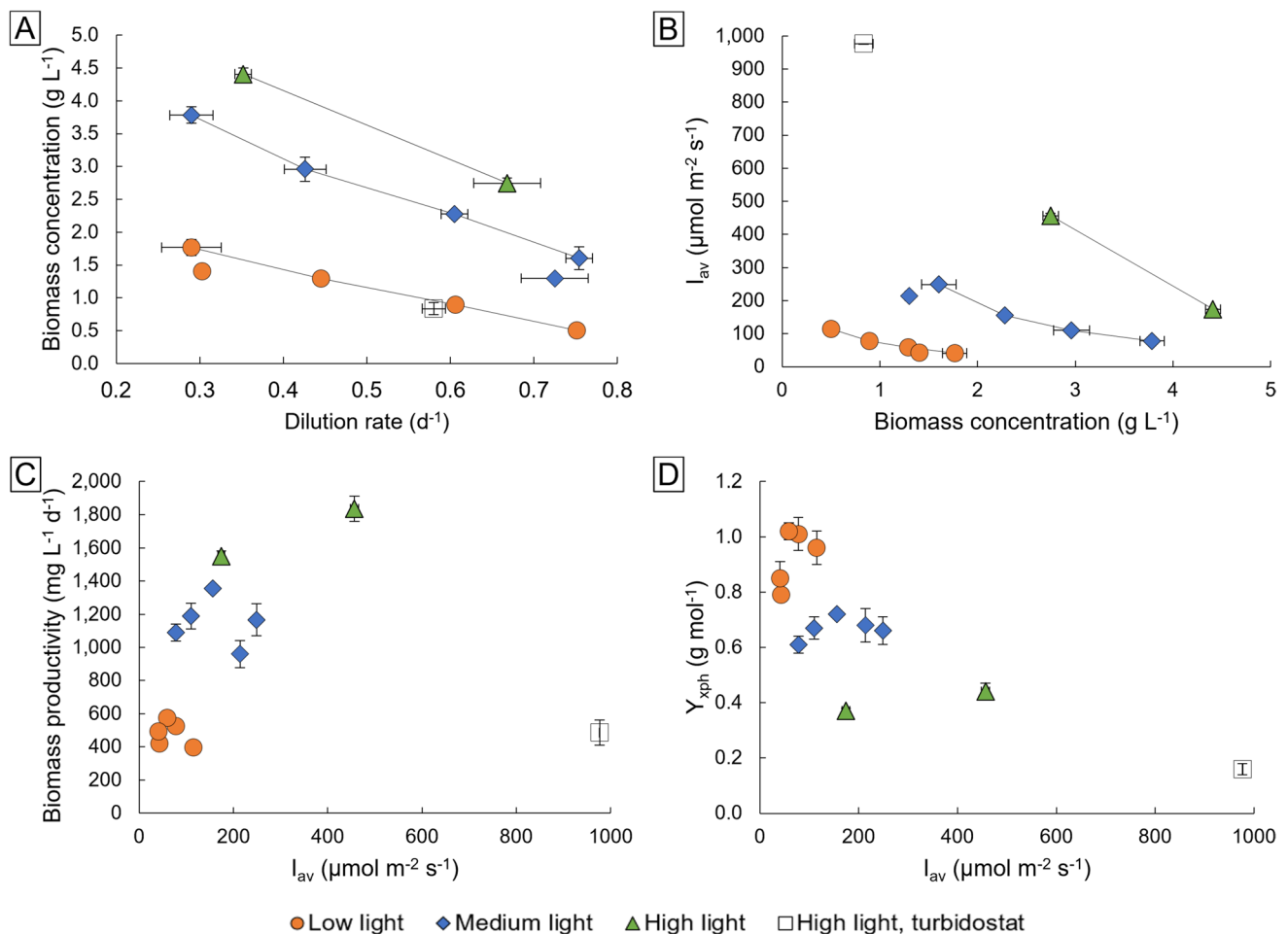


Fig. 1 (A) Biomass DW (g L⁻¹) of *N. oceanica* cyclostat experiments run at dilution rates ranging from 0.29 to 0.81 day⁻¹ for the incident light intensities (I_{ph,0}) at 200 μmol photons m⁻² s⁻¹ (LL; red; circles), 670 μmol photons m⁻² s⁻¹ (ML; blue; diamonds) and 1550 μmol photons m⁻² s⁻¹ (HL green; triangles). (B) Average light intensity (I_{av}; μmol photons m⁻² s⁻¹) at each biomass DW and I_{ph,0} tested (C) Bio-

mass productivity (mg L⁻¹ day⁻¹) and (D) biomass yield on light (g mol⁻¹) at each I_{av} and I_{ph,0}. The turbidostat experiment (HL-tbstat; white; square) was differentiated from the cyclostat experiments. Error bars indicate the standard deviation of 3 replicates at steady state collected on different days. Lines in graph A and B are added to support visualization

0.69, 0.67, and 0.66 at the lowest I_{av} to 0.67, 0.60, and 0.61 at the highest I_{av} (Table S2). When comparing this decrease in QY with the HL-tbstat findings, we can conclude that growth was minimally affected in LL, ML, and HL conditions and photoinhibition effects were negligible at the range of I_{av} tested.

Increasing the I_{ph,0} resulted in an increase in biomass productivity (r_x) with a concomitant decrease in biomass yield on light (Y_{xph}; Fig. 1C and D, Table S3). In addition, a specific I_{av} could be observed where r_x and Y_{xph} were optimal for each incident light intensity. The optimal r_x and Y_{xph} were found at a higher I_{av} value when incidental light intensities were increased. Similar observations were described in chemostat experiments with *Arthrospira platensis*, where optimal r_x increased as biomass concentrations and incidental light intensities increased (Qiang & Richmond 1996).

Increasing the biomass concentration in the reactor modulates the light gradient and therefore the light intensity perceived by the culture. When the local light intensity falls below the compensation light setpoint (I_{ph,c}), dark zones appear in the reactor where respiratory processes predominate. The optimal productivity is found when the reactor operates with an outgoing light intensity (I_{ph,d}) equal to the specific I_{ph,c} of the microalga (Takache et al. 2010; Janssen 2016). Dedicated experiments with *Nannochloropsis spp.* at low and light limiting conditions found a maintenance requirement of 3.53 mmol g_{DW}⁻¹ h⁻¹ (Barten et al. 2022) and therefore an I_{ph,c} of 4 μmol photons m⁻² s⁻¹. Assuming the a_x at low light conditions is 250 m² kg⁻¹ (described in the next section), our study confirms an I_{ph,c} of 4 μmol photons m⁻² s⁻¹. Based on this I_{ph,c} and the measured I_{ph,d} (Table S2) values, our experiments only contained dark zones at the

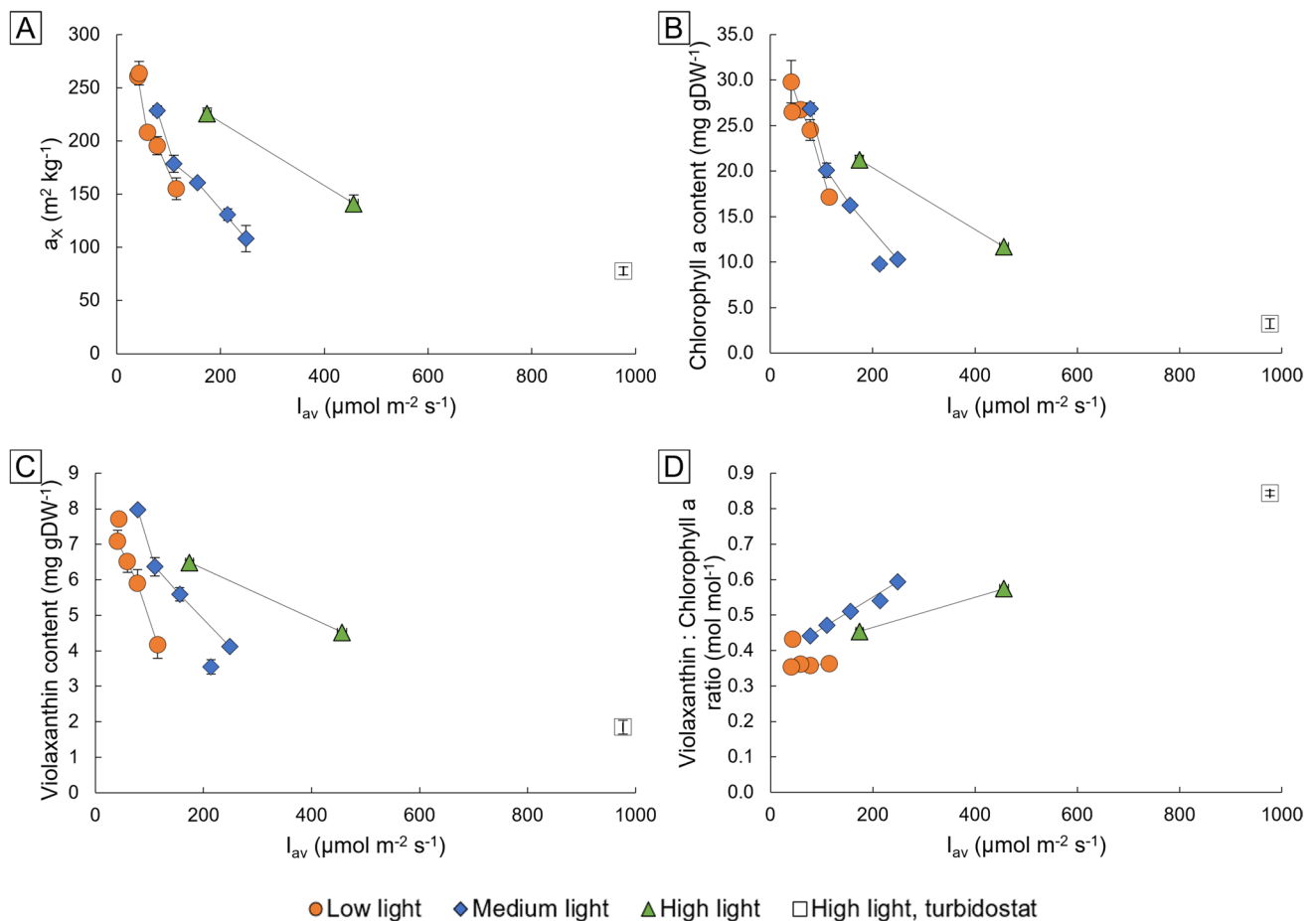


Fig. 2 (A) Averaged specific absorption cross section ($\text{m}^2 \text{kg}^{-1}$), chlorophyll a content ($\text{mg g}_{\text{DW}}^{-1}$), Violaxanthin content ($\text{mg g}_{\text{DW}}^{-1}$) and Violaxanthin-to-chlorophyll a ratio (mol mol^{-1}) as a function of the I_{av} at LL (red; circles), ML (blue; diamonds) and HL (green; triangles). Error bars indicate the standard deviation of 3 replicates collected on different days during steady state cultivation. The turbidostat experiment (HL-tbstat; white; square) is indicated separately from the cyclostat experiments

observed at higher incident light intensities. The decrease in yield was especially severe in the HL-turbidostat setup, due to the high I_{av} of the experiment. Under those conditions, the Y_{xph} decreased by 64% compared to the optimal Y_{xph} found at HL. The Y_{xph} decreased less (15%) at an increased biomass concentration, despite the occurrence of dark zones. Overall, our results support previous theoretical and experimental observations (Qiang & Richmond 1996; Olivieri et al. 2015; Pfaffinger et al. 2016; Loomba et al. 2021) that increasing the biomass concentration alleviates growth-impairing effects at over-saturating incident light conditions.

lowest D of all light conditions, and at the second lowest D in the ML condition. A dark zone can be defined through the illuminated fraction (ϵ), which accounts for the fraction of photic zones over the reactor depth. We found an ϵ of 0.78 and 0.87 for the duplicates at LL, 0.88 and 0.62 for the two dilution rates at ML, and 0.69 for the HL. Consequently, the biomass productivity decreased by 11% and 23% for the LL, 4% (D of 0.43), and 12% (D of 0.29) for the ML, and 16% for the HL, compared to the optimal productivities found in each condition. Except for one of the replicates at LL, our results are in agreement with previous results indicating that a 15% reduction in the ϵ simply decreased the r_x by 10% (Takache et al. 2010).

On the contrary, decreasing the cell concentration at higher $I_{\text{ph},0}$ exposes cells to increased over-saturating light conditions in the photic zone. As a result, more energy from light absorption is dissipated as heat instead of being channeled into photochemistry, and therefore lower Y_{xph} values are reached. This hypothesis supports the lower optimal Y_{xph}

Effect of incident light and light gradients on photosynthetic absorption and pigment composition

Cells adjust their pigmentation and absorption capacity to the light regime that they experience. Given this acclimation property, we can measure the specific absorption cross

section (a_x) to gain insight into how cells respond to different incident and average light intensities (Fig 2A). A decrease in a_x was observed as I_{av} increased under each incident light condition, reflecting the culture's adaptation to high light conditions. When moving from the lowest I_{av} to the highest I_{av} settings, the cyclostat cultures adjusted by reducing the a_x by 40%, 51%, and 37% at LL, ML, and HL respectively. An even larger decrease in a_x (65%) was measured for the HL-turbidostat experiment compared to the lowest HL I_{av} setting, as a result of the photoinhibition induced at this extreme light condition.

Alterations in the a_x are caused by a re-organisation of the antenna complexes in the thylakoid membranes. Photosystems in *Nannochloropsis* species contain chlorophyll *a* (Chl *a*) and lack chlorophyll *b* and *c*. Additionally, light-harvesting complexes contain unusual contents of violaxanthin (Viol) and vaucherixanthin structured in violaxanthin-chlorophyll protein (VCP) complexes (Lubián et al. 2000; Basso et al. 2014). The xanthophylls Viol and vaucherixanthin can be converted to antheraxanthin and zeaxanthin at photosaturating and photoinhibiting conditions, which protect the photosynthetic apparatus through quenching. Thus, Chl *a* and Viol contents were measured together with other minor carotenoids found in *N. oceanica* (Fig 2B and C; Table S4) to assess the underlying effects of the light regime on photoprotection. Similar to the a_x , both Chl *a* and Viol content decreased with increasing I_{av} and $I_{ph,0}$. The Chl *a* content decreased 42%, 62%, and 45% from the lowest to the highest I_{av} at LL, ML, and HL respectively for the cyclostat experiments, while Viol decreased 41%, 48%, and 30%. When comparing the HL-tbstat experiment with the HL cyclostat experiment at the lowest I_{av} , the decrease was 85% and 71% for Chl *a* and Viol, indicating the stress to which cells were subjected. The ratio of Viol to Chl *a* was calculated to evaluate photosaturation or photoinhibition effects (Fig 2D). Except for the replicate experiment, the ratio Viol/Chl *a* did not change at LL indicating that cultures experienced little photosaturation effects under this condition. However, at ML and HL, the ratio was not only higher than at LL but also increased with the I_{av} . The increasing Viol/Chl *a* ratios support the activation of photoprotective mechanisms to dissipate the excess absorbed energy as heat (Liu et al. 2019). At HL and I_{av} 976 $\mu\text{mol photons m}^{-2} \text{s}^{-1}$ the ratio was the highest (0.85) indicating a strong photoinhibitory effect. Besides the low QY (0.44), the content of zeaxanthin was also the highest observed (0.38 $\text{mg g}_{\text{DW}}^{-1}$; Table S4). Zeaxanthin and antheraxanthin are xanthophylls derived from the de-epoxidation of violaxanthin by violaxanthin de-epoxidase (VDE) when there is an excess of light. They are involved in the photoprotection of the photosystems by quenching the excess of the absorbed light and scavenging ROS. Zeaxanthin specifically contributes to the non-photochemical quenching with the activation

of the energy-dependent quenching q_E or the irreversible quenching q_Z (Dall'Osto et al. 2012; Liu et al. 2019).

Interestingly, the a_x was higher at similar I_{av} and increasing $I_{ph,0}$, suggesting the light gradient positively affects the a_x . For instance, the a_x was 226 and 161 $\text{m}^2 \text{kg}^{-1}$ at similar I_{av} values of 174 and 156 $\mu\text{mol photons m}^{-2} \text{s}^{-1}$, at HL and ML, respectively. As previously explained, the illuminated fraction shifts as I_{av} is kept stable and $I_{ph,0}$ varies. The occurrence of dark zones at similar I_{av} and increasing $I_{ph,0}$ corresponds with increasing biomass concentrations, limiting the available light for growth. To maximise light capture, a_x and QY are increased (from 0.63 to 0.66) with a concomitant twofold decrease in the Y_{xph} (0.72 to 0.37). Similar pigmentation effects were observed with *Dunaliella tertiolecta* in L/D flashing cycles, where a higher a_x at saturating incident light intensities also did not translate into an improvement in photosynthetic efficiency (Janssen et al. 2001).

The decrease in Y_{xph} can be mainly explained by the cost of a high a_x at a steep light gradient. First of all, photoacclimation is an energy-demanding process involving the synthesis of membrane proteins and pigments including their post-assembly into photosynthetic complexes. Expanding the cell membrane surface, and thus the absorption area, consumes energy that could otherwise be used for growth purposes. Secondly, the steep light gradient requires high levels of energy dissipation. Non-photochemical quenching is activated at even moderately high incident light intensities. At HL, the light gradient was steeper than at ML indicating that a notable reactor volume was at high-saturating light conditions. Therefore, the experiment at HL combined regions with light below the $I_{ph,c}$ where respiration is frequent, with regions with high light conditions where non-photochemical quenching is likely to occur. The activation of different forms of energy dissipation can severely influence productivity despite the cultures being acclimated to high light (de Mooij et al. 2017). In steep light gradient conditions, a high a_x is undesirable since it accentuates the over-saturation effects experienced at high incident light intensities. Overall, although increasing the biomass concentration at high $I_{ph,0}$ could be a beneficial strategy to achieve high productivities, it results in an unfavourable acclimation that results in lower photosynthetic efficiencies.

Effect of incident light and light gradients on polar and neutral lipid contents

Light triggers changes in both the content of lipid classes and the FA composition (Simionato et al. 2011; Alboresi et al. 2016). The effect of the light regime has been extensively studied in optically thin cultures, but the effect derived from the light gradient originating from dense cultures has been less investigated, especially in long-term acclimated cultures. Our study shows a linear increase of

TFA content with the average light intensity, from 11 to 15% w/w and 12 to 18% w/w at LL and ML, respectively (Fig S4). At HL, a similar linear increase is seen up to 15.5% w/w TFA, which stagnated at 16% at I_{av} greater than $456 \mu\text{mol photons m}^{-2} \text{s}^{-1}$. In such light conditions, lipid production is inhibited, as evidenced by the lower dilution rate and the reduced TFA content found at $976 \mu\text{mol photons m}^{-2} \text{s}^{-1}$ compared to $448 \mu\text{mol photons m}^{-2} \text{s}^{-1}$ (Fig S4). It was previously reported that lipid synthesis is down-regulated in the chloroplast under highly saturating light conditions (Alboresi et al. 2016).

Total lipids can be classified into polar and neutral lipids. Polar lipids in *Nannochloropsis* comprise phospholipids, glycolipids, and betaine lipids, while neutral lipids comprise triacylglycerols (TAG), diacylglycerols (DAG), and free fatty acids (FFA). At very low I_{av} , and for the different $I_{ph,0}$, 60–80% of the FAs were allocated to the polar fraction (Fig 3A and B). At LL, ML, and HL, the polar lipids decreased at increasing I_{av} from 9.0 to 6.5% w/w, 8.5 to 6.5% w/w, and 8.3 to 5.3% w/w, respectively. The decrease in polar lipids is mainly due to a decrease in glycolipids while no change in phospholipids and betaine lipids was observed (Fig 3C, D, E; Fig S5). Glycolipids, including monogalactosyldiacylglycerol (MGDG), digalactosyldiacylglycerol (DGDG), and sulfoquinovosyldiacylglycerol (SQDG), constitute the most abundant lipid classes in plants due to their high presence in the plastid membranes and their relevance in photosynthesis (Sukenic et al. 1991). Glycolipids decreased from 5.1 to 3.1% w/w at LL and ML, and from 4.5 to 2.1% w/w at HL, thus indicating a photoinhibition effect both at high $I_{ph,0}$ and I_{av} . The decrease in glycolipids is in agreement with the decrease in specific absorption cross-section and pigmentation content, as described above. From the glycolipids, MGDG showed the most considerable decrease at high I_{av} (2.6 to 1.1% w/w, 2.5 to 1.3% w/w, and 2.1 to 0.5% w/w at LL, ML, and HL, respectively), followed by DGDG (1.4 to 1.3% w/w, 1.4 to 1.2% w/w and 1.3 to 1% w/w at LL, ML, and HL, respectively) and SQDG (1.0 to 0.7, 1.0 to 0.8 and 1.1 to 0.7 w/w at LL, ML, and HL, respectively) (Fig S5).

From the phospholipids, only phosphatidylglycerol (PG) showed a significant decrease at high I_{av} at ML and HL from 0.7 to 0.5% w/w and HL 0.8 to 0.5% w/w, respectively (Fig S5). TAG was the lipid class that showed the biggest change from low to high I_{av} . At LL, the content increased from 2.2 to 7.3% w/w, whereas at ML and HL it increased from 3.1 to 11.1% w/w and 3.4 to 10.2% w/w, respectively. DAG and FFA were also measured and their contents increased approximately from 0.2 to 0.4% w/w (Fig S5). Nevertheless, the analytical error of the TLC separation for these two lipid classes was shown to be very high (Figure S1). The high deviation found by the method could lead

to the appearance of outliers, such as the ones found at ML (FigS5).

The acclimation process to high or low light conditions not only involves changes in the pigmentation but also in the lipid class composition. MGDG is a galactolipid whose conical shape facilitates the formation of non-bilayer structures namely hexagonal (H_{II}) phase or cubic phase, while DGDG and SQDG are lipid species with a cylindrical shape that facilitate the formation of bilayers or lamellar phases. While lamellar phases have a structural role, H_{II} phases are very relevant for certain enzymatic activities such as the de-epoxidation of violaxanthin (Jouhet 2013; Seiwert et al. 2018). Under low light conditions, in which maximal absorption area is required, the thylakoid surface is increased owing to the formation of grana stacks. MGDG facilitates stack formation by inducing intrinsic curvatures within the lamellar bilayer structure. The degree of grana stacking can be assessed by the MGDG: DGDG ratio. A high ratio indicates a high degree of membrane stacking while a low ratio indicates a high predominance of lamellar structures (Demé et al. 2014). Our results show that the MGDG: DGDG ratio decreased from 1.7 to a minimal value of 0.7, indicating changes from hexagonal to lamellar structures when moving from lower to higher average light intensities.

Previous studies in *Nannochloropsis* species showed that MGDG and TAG were the main lipid classes changing in content under different light conditions (Sukenic et al. 1989; Alboresi et al. 2016; Han et al. 2017). However, there is less consistency in the literature on how light conditions affect the other lipid classes. A clear example is the lipid class diacylglyceryltrimethylhomo-serine (DGTS), which responded differently under various light conditions. A more than twofold increase in the DGTS content was observed in *Nannochloropsis gaditana* when grown under 10 compared to $1000 \mu\text{mol photons m}^{-2} \text{s}^{-1}$ (Alboresi et al. 2016). In a different study, the DGTS content decreased almost twofold in *Nannochloropsis oceanica* when grown in 50 compared to $200 \mu\text{mol photons m}^{-2} \text{s}^{-1}$ (Han et al. 2017). DGTS is a betaine lipid highly present in microalgae, in comparison to higher plants, and far less studied compared to other polar lipid classes due to its late discovery (Brown & Elovson 1974; Canāvate et al. 2016). It is located in the endoplasmic reticulum and plays a pivotal role as a substitute for phosphatidylcholine (PC) under phosphate starvation (Mühlroth et al. 2017) and adaptation to cold temperatures (Murakami et al. 2018). Contrary to observations from Alboresi et al. (2016), in our study DGTS content remained relatively constant and only decreased when photoinhibition became present at highly saturating light conditions.

Similar to DGTS, both PC and PG were previously shown to decrease by twofold when moving *Nannochloropsis* species from low to high light conditions (Alboresi et al. 2016; Han et al. 2017). In our work, both PC and PG maximally

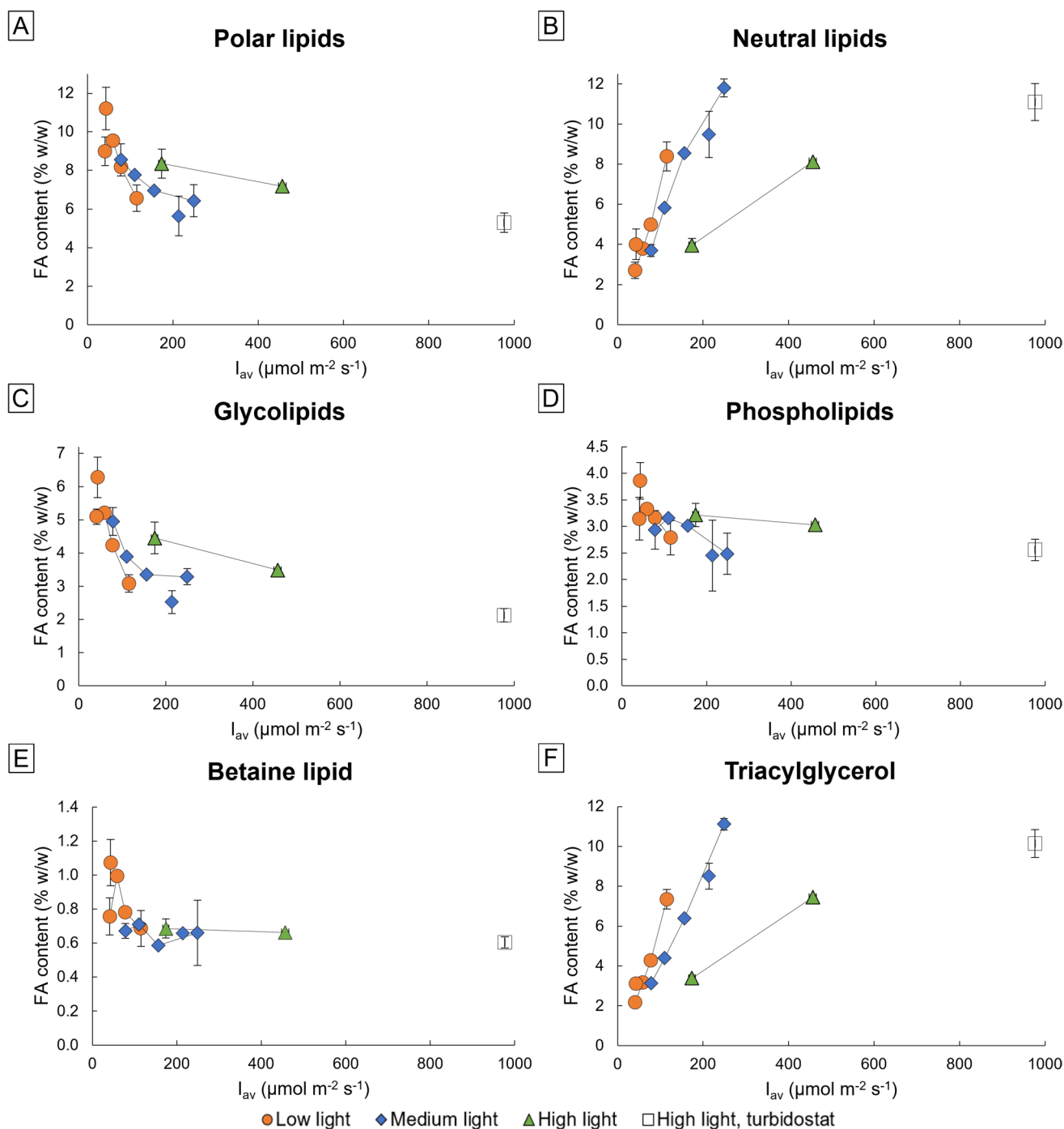


Fig. 3 Distribution of TFA between (A) polar (PL) and (B) neutral (NL) fractions over average light intensity at LL (red circles), ML (blue diamonds) and HL (green triangles). FA content (% w/w) in (C)

glycolipids, (D) phospholipids, (E) the betaine lipid DGTS, and (F) triacylglycerols. Error bars indicate the standard deviation of 3 different replicates at steady state collected on different days

decreased by 1.58- and 1.28-fold, respectively, across all light conditions.

This divergence between previous work and our studies could lie in the variations in experimental setup, analysis methodology, or even in differences between genera. Previous studies cultivated *Nannochloropsis* in batch conditions,

therefore the differences in PG and PC decrease might be due to differences between long-term and short-term acclimated cultures. Even differences in genera could explain these deviations, since *N. gaditana* was recently reclassified as *Microchloropsis gaditana* (Fawley et al. 2015). Another divergence with literature could lie in the methodologies

used for lipid class analysis. TLC fractionation was commonly used in the past for unveiling the lipid profile of microalgae whereas now technologies involving mass spectrometry (MS) are gaining relevance (Da Costa et al. 2016). MS allows for precise detection of lipid classes in very small quantities compared to TLC methods, as well as a detailed assessment at a molecular level of the different lipid classes. More specifically, information regarding the positioning and number of fatty acyl chains, the degree of desaturation, and the carbon number for the different species present for each lipid class is obtained by MS methods. However, the use of MS methods generally requires extensive optimisation of the operational conditions including the use of the proper standards (Gros & Jouhet 2018). Overall, lipidomics data at varying light conditions is still scarce in the microalgal field, but it is expected to increase in the coming years due to the continuous improvement of analytical techniques and the potential of microalgal lipid classes as bioactive compounds.

FA composition of lipid classes is affected by both incident and average light intensity.

The FA composition of the lipid classes changes along light gradients and ingoing light intensities. The changes in the FA composition of each lipid class at the different incident light intensities are represented in Fig. 4 as a heatmap. The heatmap shows the ratio between the highest I_{av} (HI_{av}) and lowest I_{av} (LI_{av}) per FA. For the HL condition, the FA composition obtained in the HL-tbstat experiment was used as HI_{av} . The absolute changes in percentages are also included in Fig S6. The method was sensitive to less frequent lipids classes, and therefore we only evaluated the most abundant ones including MGDG, DGDG, DGTS, TAG, PE, PC, and PG. From all FA's, the most substantial changes were observed in the major FAs palmitic acid (C16:0), palmitoleic acid (C16:1), arachidonic acid (C20:4), and eicosapentaenoic acid (C20:5, EPA). Similar shifts in these C16 and C20 FAs have been reported in previous studies (Sukenik et al. 1989; Alboresi et al. 2016; Han et al. 2017). Saturated fatty acids (SFAs) were constant or increased at high I_{av} . The most significant increase of SFA was shown at high I_{av} in DGTS over all $I_{ph,0}$ conditions, while TAG and PC showed an attenuated SFA increase at higher $I_{ph,0}$. Monounsaturated fatty acid (MUFA) contents remained unchanged or were generally lower at higher I_{av} for most lipid classes, except for PG which increased in MUFA. The observed increase for PG was mainly due to C16:1, which was found to be higher for all the different incident light conditions. The increase of the trans isoform of C16:1 in PG under high light conditions has been reported as a photoprotective mechanism to stabilise the trimerization of the LHC of the PSII (Dubertret et al. 2002).

Polyunsaturated fatty acid contents (PUFAs) decreased at high I_{av} for all lipid classes. An exception was formed by DGDG, where PUFA significantly increased mainly owing to the increased EPA content. The slight increase of EPA-enriched DGDG species in the thylakoid membranes supports the photoprotective role of EPA under stress light conditions (Alboresi et al. 2016). Despite no significant increase in PUFAs in the PC class was observed, a shift was seen in C18 species. Linolenic acid (C18:3) was significantly higher at high I_{av} while linoleic acid (C18:2) was significantly lower. Moreover, the PE lipid class showed increased EPA contents at high I_{av} at the expense of the PUFAs C20:4 and C18:2, with a significant increase especially at HL. The lipid class PC is known as a pool for the desaturation of C18 FA and the class PE is recognised as the desaturation pool of C20 FA (Schneider & Roessler 1994; Han et al. 2017). Our results indicate an intensification in FA desaturation at high average light intensities, possibly to fulfil the demand for desaturated species at highly saturating light conditions.

The desaturated products C20:5 (EPA) and C20:4 from PE can be converted further into DAG, which in turn serves as a precursor for the synthesis of plastidial lipids such as MGDG. In addition to PE, DGTS has been suggested to have a similar role in the synthesis of EPA, functioning as a storage depot of EPA for polar lipids (Han et al. 2017; Murakami et al. 2018). The role of a PUFA storage reserve has usually been associated with TAG under conditions such as nitrogen starvation (Solovchenko 2012; Janssen, et al. 2019a, b). In our studies, both DGTS and TAG showed a decrease of a fraction of EPA under high I_{av} compared to low I_{av} conditions. DGTS showed an EPA decrease in all $I_{ph,0}$ conditions whereas TAG only showed EPA increase at LL and ML. Similar patterns were observed for C20:4, C18:2, and C18:0 (stearic acid) for both lipid classes. The almost identical profile for the abovementioned FAs could indicate a similar role of both lipid classes under light-saturating conditions.

EPA content and distribution change with the incident and average light intensity

The polyunsaturated EPA can be located both in membrane lipids or in TAG, and the localization strongly depends on the culture conditions (Sukenik et al. 1989; Janssen et al. 2018). As shown by the lipid class analysis, shifts in lipid class contents and their fatty acid distributions result in shifting EPA contents of the biomass.

Figure 5A shows that the EPA content had a maximal relative decrease of 28% from the highest content reported at LL and I_{av} of $59 \mu\text{mol photons m}^{-2} \text{s}^{-1}$ (3.7% w/w) to the lowest content reported at HL and I_{av} of $976 \mu\text{mol photons m}^{-2} \text{s}^{-1}$ (2.8% w/w). The light gradient did not change the EPA content significantly at LL but did significantly

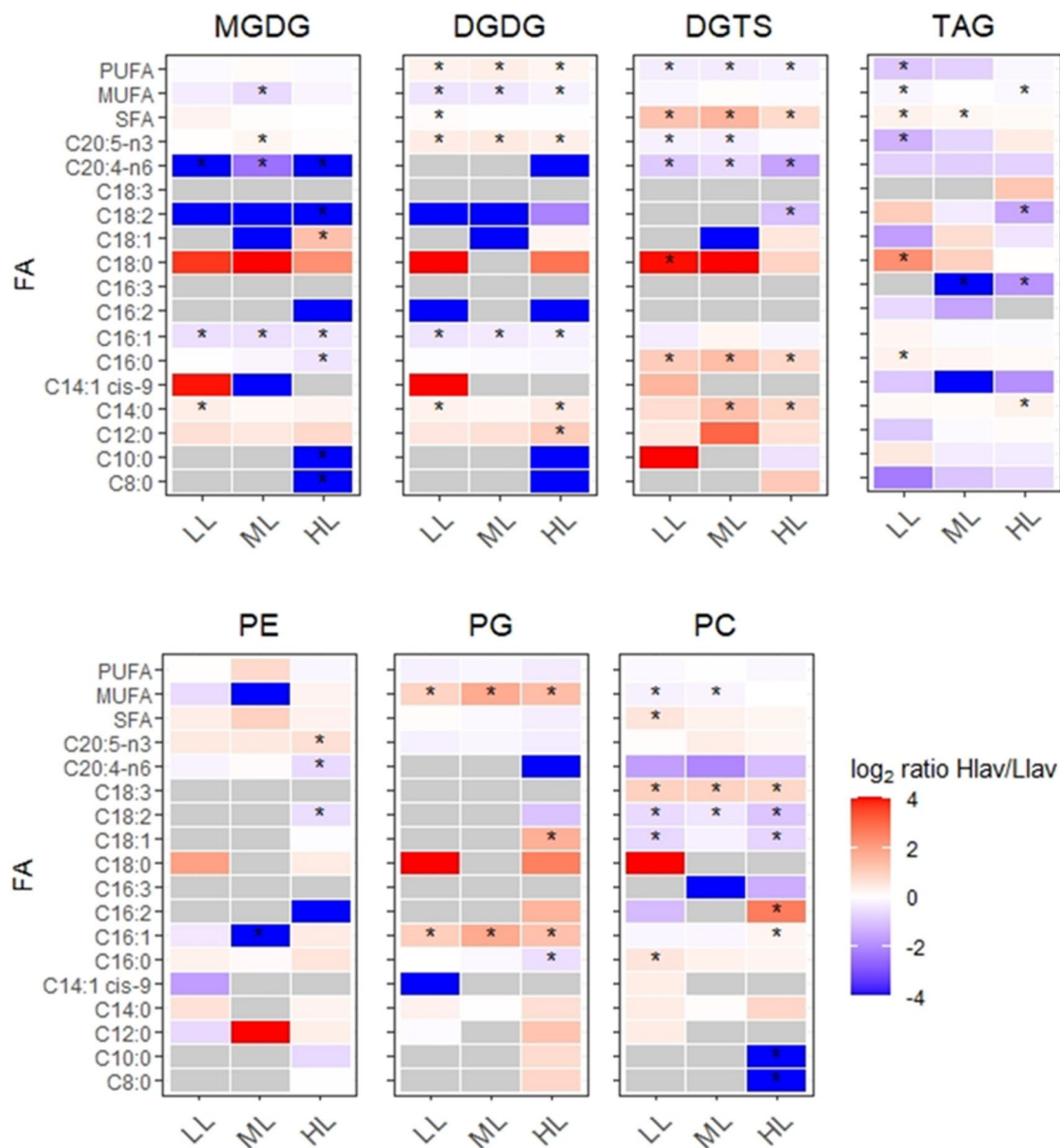


Fig. 4 Heatmap of the main lipid classes (MGDG, DGDG, DGTS, TAG, PE, PG, PC) describing the ratio of change of FA from high average light intensity (HI_{av}) compared to low average light intensity (LI_{av}) at LL, ML and HL ingoing light intensities. FAs that were not

detected both at HI_{av} and LI_{av} are coloured grey. Asterisks indicate a significant change with a p-value lower than 0.05 between HI_{av} and LI_{av} ($n=3$, except for PE, in which one replicate was detected as an outlier and therefore omitted from this analysis)

decrease EPA content at ML and HL. At LL, the EPA content remained constant at 3.4% w/w. However, at higher $I_{ph,0}$ in ML and HL, the total EPA content decreased respectively from 3.6 to 3.1% w/w (ANOVA, $p < 0.01$), and 3.4 to 2.8% w/w (ANOVA, $p < 0.01$) from the lowest to the highest I_{av} .

Besides affecting the total EPA content of the biomass, the I_{av} also influenced EPA distribution between polar and neutral fractions (Fig 5B). EPA in the polar fraction decreased from 3.0% w/w at the lowest applied I_{av} to 2.6, 2.5, and 2.0% w/w at the highest I_{av} at LL, ML, and HL respectively. Simultaneously, EPA in the neutral fraction

increased from 0.4 to 0.9, 0.8, and 1.1% w/w in the respective incident light conditions. The decrease of EPA in the polar fraction at high I_{av} is mainly explained by the decrease in the MGDG content, whereas the EPA increase in the neutral fraction mirrors the increase in TAG. Both changes in lipid class contents resulted in an overall decrease in EPA on a total lipid basis (Fig S7). Under all applied light conditions in this study, the highest percentage of EPA in the total lipid fraction was attained at the lowest I_{av} at the LL conditions (27–30%) decreasing with increasing I_{av} for each $I_{ph,0}$ setting (17–23%).

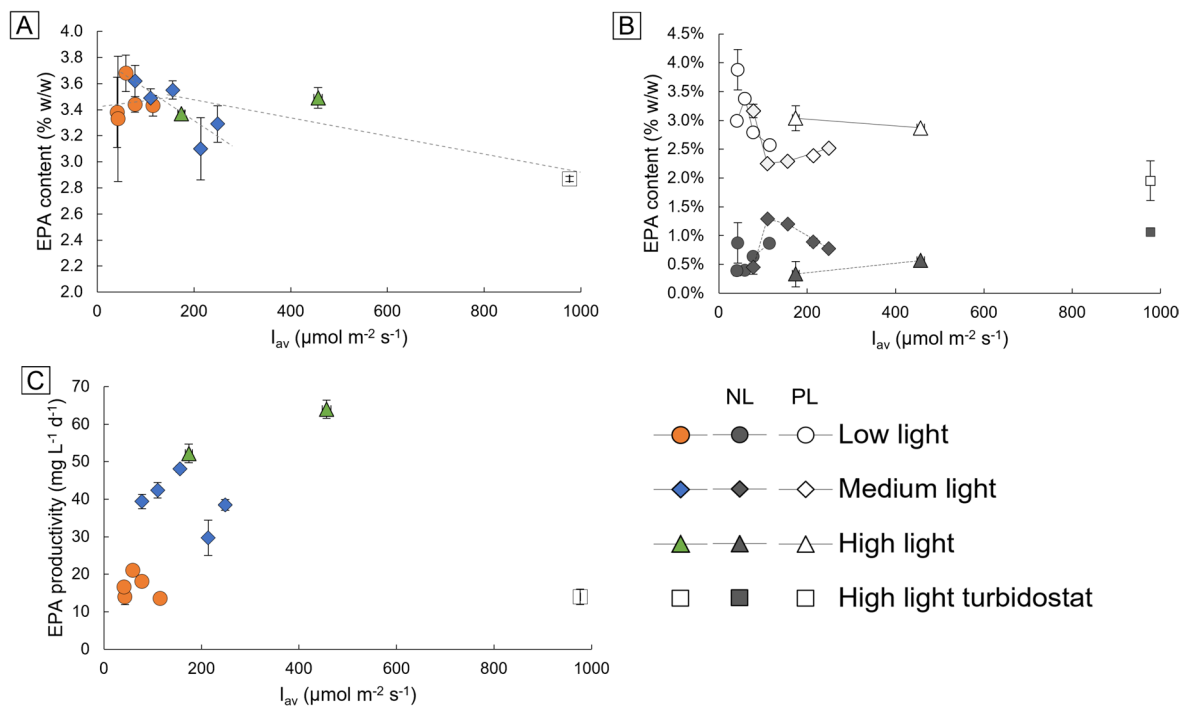


Fig. 5 (A) EPA content (% w/w), (B) distribution of EPA between polar and neutral fractions, and (C) EPA productivity ($\text{mg L}^{-1} \text{day}^{-1}$) over the average light intensity ($\mu\text{mol photons m}^{-2} \text{s}^{-1}$) at LL (red circles), ML (blue diamonds) and HL (green triangles). Squared data points represent a separate experiment done in turbidostat. Black and

white markings were used to distinguish between the polar and the neutral fraction. Error bars represent the standard deviation of three replicates. Graph lines in A and C are derived from a linear and polynomial model, while in B only connects the data points to help visualisation

Moreover, EPA productivities at increasing I_{av} were calculated (Fig 5C). Similar to biomass productivity, EPA productivity also increased depending on both the $I_{ph,0}$ and the I_{av} . The optimal EPA productivity coincided with the I_{av} that resulted in an optimal biomass productivity. This finding supports previous observations that optimal conditions for EPA production are found at optimal conditions for biomass production (Sukenik 1991; Zou et al. 2000; Camacho-Rodríguez et al. 2014).

Although the effect of incident light on lipid and EPA has been thoroughly studied in microalgae, the interaction between the incident light and different biomass concentrations on lipids has received less attention. Our study shows that the EPA content was affected by the average light intensity, mainly when the $I_{ph,0}$ was higher than $200 \mu\text{mol photons m}^{-2} \text{s}^{-1}$. While several studies on optically thin cultures of *Nannochloropsis* proved a decreasing effect on the EPA content at higher incoming irradiances (Sukenik et al. 1989; Sukenik 1991; Fabregas et al., 20,030, other similar studies showed only a limited effect (Chini Zittelli et al. 1999; Pal et al. 2011; Camacho-Rodríguez et al. 2014). Alternatively, a study by Zou and Richmond (2000) on ultradense cultures of *N. oculata* found that both incident and average light intensity negatively affected the EPA content, with the latter light gradient factor being more relevant. According

to our results, the EPA content was significantly affected by increasing I_{av} , especially in conditions of increased photosaturation. The lowest EPA content was observed at an I_{av} of $976 \mu\text{mol photons m}^{-2} \text{s}^{-1}$, where photoinhibition was shown to occur. Therefore, modulating the biomass concentration at variable incident light intensities can be used to influence the accumulation and especially the distribution of EPA in the polar and neutral fractions.

Conclusions

Increasing biomass concentrations in the reactor is a useful tool for coping with high incident light conditions and for achieving high biomass productivities. Nevertheless, light gradients covering light-limiting conditions and highly saturating conditions result in an inadequate acclimation response. In terms of lipids, triacylglycerols and plastidial lipids underwent the biggest changes both at high and low average light intensities. At the physiological level, changes in polar lipids affected the light absorption and the activation of non-photochemical quenching processes such as the violaxanthin cycle. The content of EPA was unaffected by the light regime at low incident light intensities while it decreased at higher average light intensities due to the

increased photosaturation. EPA, which was mainly present in the polar fraction at low average light intensities, was reduced at high average light intensities due to a decrease in plastidial lipids. A relative decrease of 28% in EPA content was observed when moving from an average light intensity of 59 to 976 $\mu\text{mol photons m}^{-2} \text{s}^{-1}$. The tight control in maintaining this polyunsaturated fatty acid between all the polar lipids classes denotes an indispensable role in coping with high incident light conditions.

Supplementary Information The online version contains supplementary material available at <https://doi.org/10.1007/s10811-024-03373-0>.

Acknowledgements The authors would like to thank Dr. Juliette Jouhet and the Laboratoire de Physiologie Cellulaire et Végétale (LPCV) for their valuable guidance in lipid class analysis.

Authors' contributions Conception and design of the paper was performed by NF-L, SvO, RHW, MJ and MJB. Analysis and interpretation of the data was done by NF-L, SvO, RHW, MJ, ITDC and MJB. The article was drafted by NF-L and SvO. Critical revision of the article for important intellectual content was performed by NF-L, SvO, RHW, WE, MJ, MJB and CS. Statistics were performed by NF-L, CS and ITDC. Funding was obtained by RHW and MJB. Technical support was provided by WE, CS and MJ. Collection and assembly of the data was performed by NF-L, SvO, WE and CS. All authors approved the final version of the article.

Funding This study was funded by the “Microalgae As a Green source for Nutritional Ingredients for Food/Feed and Ingredients for Cosmetics by cost effective New Technologies” (MAGNIFICENT) project, funded by the Bio Based Industries Joint Undertaking under the Horizon 2020 research and innovation program from the European Union (grant agreement 745754). Additional funding was obtained from the Topconsortia voor Kennis & Innovatie voor Biobased Economy (TKI-BBE) and the Algemene Neerlandsche Wielrijders Bond (ANWB) with project number TKI_BB_1802.

Data availability All data supporting the findings of this study are available within the paper and its Supplementary Information. The raw data can be accessed upon request to the authors.

Declarations

Competing interests The authors declare no competing interests.

Open Access This article is licensed under a Creative Commons Attribution 4.0 International License, which permits use, sharing, adaptation, distribution and reproduction in any medium or format, as long as you give appropriate credit to the original author(s) and the source, provide a link to the Creative Commons licence, and indicate if changes were made. The images or other third party material in this article are included in the article's Creative Commons licence, unless indicated otherwise in a credit line to the material. If material is not included in the article's Creative Commons licence and your intended use is not permitted by statutory regulation or exceeds the permitted use, you will need to obtain permission directly from the copyright holder. To view a copy of this licence, visit <http://creativecommons.org/licenses/by/4.0/>.

References

- Adarme-Vega TC, Lim DKY, Timmins M, Vernen F, Li Y, Schenk PM (2012) Microalgal biofactories: A promising approach towards sustainable omega-3 fatty acid production. *Microb Cell Facto* 11:96
- Alboresi A, Perin G, Vitolo N, Diretto G, Block M, Jouhet J, Meneghesso A, Valle G, Giuliano G, Maréchal E, Morosinotto T (2016) Light remodels lipid biosynthesis in *Nannochloropsis gaditana* by modulating carbon partitioning between organelles. *Plant Physiol* 171:2468–2482
- Al-Hoqani U, Young R, Purton S (2017) The biotechnological potential of *Nannochloropsis*. *Perspectives in Phycology* 4:1–15
- Barbosa MJ, Janssen M, Ham N, Tramper J, Wijffels RH (2003) Microalgae cultivation in air-lift reactors: Modeling biomass yield and growth rate as a function of mixing frequency. *Biotechnol Bioeng* 82:170–179
- Barten R, Chin-On R, de Vree J, van Beersum E, Wijffels RH, Barbosa MJ, Janssen M (2022) Growth parameter estimation and model simulation for three industrially relevant microalgae: *Picoclorum*, *Nannochloropsis*, and *Neochloris*. *Biotechnol Bioeng* 119:1416–1425
- Barten R, Djohan Y, Evers W, Wijffels R, Barbosa M (2021) Towards industrial production of microalgae without temperature control: The effect of diel temperature fluctuations on microalgal physiology. *J Biotechnol* 336:56–63
- Basso S, Simionato D, Gerotto C, Segalla A, Giacometti GM, Morosinotto T (2014) Characterization of the photosynthetic apparatus of the eustigmatophycean *Nannochloropsis gaditana*: Evidence of convergent evolution in the supramolecular organization of photosystem I. *Biochim Biophys Acta (BBA) - Bioenerg* 1837:306–314
- Bhatt DL, Steg PG, Miller M, Brinton EA, Jacobson TA, Ketchum SB, Doyle RT, Juliano RA, Jiao L, Granowitz C, Tardif JC, Ballantyne CM (2019) Cardiovascular risk reduction with icosapent ethyl for hypertriglyceridemia. *N Engl J Med* 380:11–22
- Breuer G, Evers WAC, de Vree JH, Kleinegris DMM, Martens DE, Wijffels RH, Lamers PP (2013) Analysis of fatty acid content and composition in microalgae. *J Vis Exp* 80:e50628
- Brown AE, Elovson J (1974) Isolation and characterization of a novel lipid, 1(3),2-diacylglyceryl-(3)-O-4'-(N,N,N-trimethyl)homoserine, from *Ochromonas danica*. *Biochemistry* 13:3476–3482
- Camacho-Rodríguez J, González-Céspedes AM, Cerón-García MC, Fernández-Sevilla JM, Ación-Fernández FG, Molina-Grima E (2014) A quantitative study of eicosapentaenoic acid (EPA) production by *Nannochloropsis gaditana* for aquaculture as a function of dilution rate, temperature and average irradiance. *Appl Microbiol Biotechnol* 98:2429–2440
- Canábate JP, Armada I, Riós JL, Hachero-Cruzado I (2016) Exploring occurrence and molecular diversity of betaine lipids across taxonomy of marine microalgae. *Phytochemistry* 124:68–78
- Chini Zittelli G, Lavista F, Bastianini A, Rodolfi L, Vincenzini M, Tredici MR (1999) Production of eicosapentaenoic acid by *Nannochloropsis* sp. cultures in outdoor tubular photobioreactors. *J Biotechnol* 70:299–312
- Da Costa E, Silva J, Mendonça SH, Abreu MH, Domingues MR (2016) Lipidomic approaches towards deciphering glycolipids from microalgae as a reservoir of bioactive lipids. *Mar Drugs* 14:27
- Dall'Osto L, Holt N. E., Kaligotla S., Fuciman M., Cazzaniga S., Carbonera D., Frank H. A., Alric J., & Bassi R. (2012) Zeaxanthin protects plant photosynthesis by modulating chlorophyll triplet yield in specific light-harvesting antenna subunits. *J Biol Chem* 287:41820–41834
- de Mooij T, Nejad ZR, van Buren L, Wijffels RH, Janssen M (2017) Effect of photoacclimation on microalgae mass culture productivity. *Algal Res* 22:56–67

- de Vree JH, Bosma R, Wieggers R, Gegic S, Janssen M, Barbosa MJ, Wijffels RH (2016) Turbidostat operation of outdoor pilot-scale photobioreactors. *Algal Res* 18:198–208
- Demé B, Cataye C, Block MA, Maréchal E, Jouhet J (2014) Contribution of galactoglycerolipids to the 3-dimensional architecture of thylakoids. *FASEB J* 28:3373–3383
- Draaisma RB, Wijffels RH, Slegers PM, Brentner LB, Roy A, Barbosa MJ (2013) Food commodities from microalgae. *Curr Opin Biotechnol* 24:169–177
- Dubertret G, Gerard-Hirne C, Trémolières A (2002) Importance of trans- Δ 3-hexadecenoic acid containing phosphatidylglycerol in the formation of the trimeric light-harvesting complex in *Chlamydomonas*. *Plant Physiol Biochem* 40:829–836
- Dyall SC, Michael-Titus AT (2008) Neurological benefits of omega-3 fatty acids. *Neuromol Med* 10:219–235
- Enzing C, Ploeg M, Barbosa MJ, Sijtsma L (eds) (2014) Microalgae-based products for the food and feed sector: An outlook for Europe. EUR 26255. Publications Office of the European Union, Luxembourg. JRC85709, 82 p
- Fabregas J, Maseda A, Dominguez A, Otero A (2003) The cell composition of *Nannochloropsis* sp. Changes under different irradiances in semicontinuous culture. *World J Microbiol Biotechnol* 20:31–35
- Fawley MW, Jameson I, Fawley KP (2015) The phylogeny of the genus *Nannochloropsis* (Monodopsidaceae, Eustigmatophyceae), with descriptions of *N. australis* sp. nov. and *Microchloropsis* gen. nov. *Phycologia* 54:545–552
- Fisher T, Minnaard J, Dubinsky Z (1996) Photoacclimation in the marine alga *Nannochloropsis* sp. (Eustigmatophyte): A kinetic study. *J Plankton Res* 18:1797–1818
- Gong Y, Kang NK, Kim YU, Wang Z, Wei L, Xin Y, Shen C, Wang Q, You W, Lim JM, Jeong SW, Park YI, Oh HM, Pan K, Poliner E, Yang G, Li-Beisson Y, Li Y, Hu Q, Poetsch A, Farre EM, Chang YK, Jeong WJ, Jeong BR, Xu J (2020) The NanDeSyn database for *Nannochloropsis* systems and synthetic biology. *Plant J* 104:1736–1745
- Griffiths MJ, Harrison STL (2009) Lipid productivity as a key characteristic for choosing algal species for biodiesel production. *J Appl Phycol* 21:493–507
- Molina Grima E, Fernández FGA, García Camacho F, Chisti Y, (1999) Photobioreactors: light regime, mass transfer, and scaleup. *J Biotechnol* 70:231–247
- Gros V, Jouhet J (2018) Quantitative assessment of the chloroplast lipidome. *Meth Mol Biol* 1829:241–252
- Guschina IA, Harwood JL (2006) Lipids and lipid metabolism in eukaryotic algae. *Prog Lipid Res* 45:160–186
- Han D, Jia J, Li J, Sommerfeld M, Xu J, Hu Q (2017) Metabolic remodeling of membrane glycerolipids in the microalga *Nannochloropsis oceanica* under nitrogen deprivation. *Front Marine Sci* 4:242
- Hess SK, Lepetit B, Kroth PG, Mecking S (2018) Production of chemicals from microalgae lipids – status and perspectives. *Eur J Lipid Sci Technol* 120:152
- Hu Q, Sommerfeld M, Jarvis E, Ghirardi M, Posewitz M, Seibert M, Darzins A (2008) Microalgal triacylglycerols as feedstocks for biofuel production: Perspectives and advances. *Plant J* 54:621–639
- Janssen JH, Driessen JLSP, Lamers PP, Wijffels RH, Barbosa MJ (2018) Effect of initial biomass-specific photon supply rate on fatty acid accumulation in nitrogen depleted *Nannochloropsis gaditana* under simulated outdoor light conditions. *Algal Res* 35:595–601
- Janssen JH, Lamers PP, de Vos RCH, Wijffels RH, Barbosa MJ (2019a) Translocation and de novo synthesis of eicosapentaenoic acid (EPA) during nitrogen starvation in *Nannochloropsis gaditana*. *Algal Res* 37:138–144
- Janssen JH, Wijffels RH, Barbosa MJ (2019b) Lipid production in *Nannochloropsis gaditana* during nitrogen starvation. *Biology* 8:5
- Janssen M (2016) Microalgal photosynthesis and growth in mass culture. In: Legrand J (Ed.) *Advances in Chemical Engineering: Photobioreactor Engineering*, Vol. 48. Elsevier, Amsterdam, pp. 185–256
- Janssen M, De Bresser L, Baijens T, Tramper J, Mur LR, Snel JFH, Wijffels RH (2000) Scale-up aspects of photobioreactors: Effects of mixing-induced light/dark cycles. *J Appl Phycol* 12:225–237
- Janssen M, Slenders P, Tramper J, Mur LR, Wijffels RH (2001) Photosynthetic efficiency of *Dunaliella tertiolecta* under short light/dark cycles. *Enz Microb Technol* 29:298–305
- Jeffrey SW, Mantoura RFC, Wright SW (1997) *Phytoplankton pigments in oceanography: Guidelines to modern methods*. UNESCO Publishing, Paris
- Jenkins DJA, Sievenpiper JL, Pauly D, Sumaila UR, Kendall CWC, Mowat FM (2009) Are dietary recommendations for the use of fish oils sustainable? *Can Med Assoc J* 180:633–637
- Jouhet J (2013) Importance of the hexagonal lipid phase in biological membrane organization. *Front Plant Sci* 4:494
- Keşan G, Litvín R, Břina D, Dürchan M, Šlouf V, Polívka T (2016) Efficient light-harvesting using non-carbonyl carotenoids: Energy transfer dynamics in the VCP complex from *Nannochloropsis oceanica*. *Biochim Biophys Acta (BBA) - Bioenerget* 1857: 370–379
- Kirchhoff H, Mukherjee U, Galla HJ (2002) Molecular architecture of the thylakoid membrane: Lipid diffusion space for plastoquinone. *Biochemistry* 41:4872–4882
- Koller AP, Wolf L, Weuster-Botz D (2017) Reaction engineering analysis of *Scenedesmus ovalternus* in a flat-plate gas-lift photobioreactor. *Bioresour Technol* 225:165–174
- Li-Beisson Y, Thelen JJ, Fedosejevs E, Harwood JL (2019) The lipid biochemistry of eukaryotic algae. *Prog Lipid Res* 74:31–68
- Liu J, Lu Y, Hua W, Last RL (2019) A new light on Photosystem II maintenance in oxygenic photosynthesis. *Front Plant Sci* 10:975
- Loomba V, von Lieres E, Huber G (2021) How do operational and design parameters effect biomass productivity in a flat-panel photo-bioreactor? A computational analysis. *Processes* 9:1387
- Lubián LM, Montero O, Moreno-Garrido I, Huertas IE, Sobrino C, González-Del Valle M, Parés G (2000) *Nannochloropsis* (Eustigmatophyceae) as source of commercially valuable pigments. *J Appl Phycol* 12:249–255
- Molina Grima E, Fernández Sevilla JM, Sánchez Pérez JA, Garcia Gamacho F (1996) A study on simultaneous photolimitation and photoinhibition in dense microalgal cultures taking into account incident and averaged irradiances. *J Biotechnol* 45:59–69
- Mühlroth A, Winge P, El Assimi A, Jouhet J, Maréchal E, Hohmann-Marriott MF, Vadstein O, Bonesa AM (2017) Mechanisms of phosphorus acquisition and lipid class remodeling under P limitation in a marine microalga. *Plant Physiol* 175:1543–1559
- Murakami H, Nobusawa T, Hori K, Shimojima M, Ohta H (2018) Betaine lipid is crucial for adapting to low temperature and phosphate deficiency in *Nannochloropsis*. *Plant Physiol* 177:181–193
- Naduthodi MIS, Barbosa MJ, van der Oost J (2018) Progress of CRISPR-Cas based genome editing in photosynthetic microbes. *Biotechnol J* 13:1700591
- Olivieri G, Gargiulo L, Lettieri P, Mazzei L, Salatino P, Marzocchella A (2015) Photobioreactors for microalgal cultures: A Lagrangian model coupling hydrodynamics and kinetics. *Biotechnol Prog* 31:1259–1272
- Pal D, Khozin-Goldberg I, Cohen Z, Boussiba S (2011) The effect of light, salinity, and nitrogen availability on lipid production by *Nannochloropsis* sp. *Appl Microbiol Biotechnol* 90:1429–1441

- Pfaffinger CE, Schöne D, Trunz S, Löwe H, Weuster-Botz D (2016) Model-based optimization of microalgae areal productivity in flat-plate gas-lift photobioreactors. *Algal Res* 20:153–163
- Polle JEW, Melis A (1999) Recovery of the photosynthetic apparatus from photoinhibition during dark incubation of the green alga *Dunaliella salina*. *Aust J Plant Physiol* 26:679–686
- Pribil M, Labs M, Leister D (2014) Structure and dynamics of thylakoids in land plants. *J Exp Bot* 65:1955–1972
- Qiang H, Richmond A (1996) Productivity and photosynthetic efficiency of *Spirulina platensis* as affected by light intensity, algal density and rate of mixing in a flat plate photobioreactor. *J Appl Phycol* 8:139–145
- Rabe AE, Benoit RJ (1962) Mean light intensity—A useful concept in correlating growth rates of dense cultures of microalgae. *Biotechnol Bioeng* 4:377–390
- Renaud SM, Parry DL, Thinh LV, Kuo C, Padovan A, Sammy N (1991) Effect of light intensity on the proximate biochemical and fatty acid composition of *Isochrysis* sp. and *Nannochloropsis oculata* for use in tropical aquaculture. *J Appl Phycol* 3:43–53
- Richmond A, Hu, Q (eds) (2013) *Handbook of microalgal culture: applied phycology and biotechnology*, 2nd edn. John Wiley and Sons
- Schneider JC, Roessler P (1994) Radiolabeling Studies of lipids and fatty acids in *Nannochloropsis* (Eustigmatophyceae), an oleaginous marine alga. *J Phycol* 30:594–598
- Seiwert D, Witt H, Ritz S, Janshoff A, Paulsen H (2018) The nonbilayer lipid MGDG and the major light-harvesting complex (LHCII) promote membrane stacking in supported lipid bilayers. *Biochemistry* 57:2278–2288
- Sijtsma L, De Swaaf ME (2004) Biotechnological production and applications of the ω -3 polyunsaturated fatty acid docosahexaenoic acid. *Appl Microbiol Biotechnol* 64:146–153
- Simionato D, Sforza E, Corteggiani Carpinelli E, Bertuccio A, Giacometti GM, Morosinotto T (2011) Acclimation of *Nannochloropsis gaditana* to different illumination regimes: Effects on lipids accumulation. *Bioresour Technol* 102:6026–6032
- Solovchenko AE (2012) Physiological role of neutral lipid accumulation in eukaryotic microalgae under stresses. *Russ J Plant Physiol* 59:167–176
- Staehelin LA (2003) Chloroplast structure: From chlorophyll granules to supra-molecular architecture of thylakoid membranes. *Photosynth Res* 76:185–196
- Sukenik A (1991) Ecophysiological considerations in the optimization of eicosapentaenoic acid production by *Nannochloropsis* sp. (Eustigmatophyceae). *Bioresour Technol* 35:263–269
- Sukenik A, Carmeli Y, Berner T (1989) Regulation of fatty acid composition by irradiance level in the eustigmatophyte *Nannochloropsis* sp. *J Phycol* 25:686–692
- Sukenik A, Zmora O, Carmeli Y (1993) Biochemical quality of marine unicellular algae with special emphasis on lipid composition. II *Nannochloropsis* sp. *Aquaculture* 117:313–326
- Takache H, Christophe G, Cornet J, Pruvost J (2010) Experimental and theoretical assessment of maximum productivities for the microalgae *Chlamydomonas reinhardtii* in two different geometries of photobioreactors. *Biotechnol Prog* 26:431–440
- Traversier M, Gaslonde T, Milesi S, Michel S, Delannay E (2018) Polar lipids in cosmetics: Recent trends in extraction, separation, analysis and main applications. *Phytochem Rev* 17:1179–1210
- Zou N, Richmond A (2000) Light-path length and population density in photoacclimation of *Nannochloropsis* sp. (Eustigmatophyceae). *J Appl Phycol* 12:349–354
- Zou N, Zhang C, Cohen Z, Richmond A (2000) Production of cell mass and eicosapentaenoic acid (epa) in ultrahigh cell density cultures of *Nannochloropsis* sp. (Eustigmatophyceae). *Eur J Phycol* 35:127–133

Publisher's Note Springer Nature remains neutral with regard to jurisdictional claims in published maps and institutional affiliations.